

Use of Replication-Conditional Adenovirus as a Helper System to Enhance Delivery of P450 Prodrug-Activation Genes for Cancer Therapy

Youssef Jounaidi and David J. Waxman

Division of Cell and Molecular Biology, Department of Biology, Boston University, Boston, Massachusetts

ABSTRACT

Cytochrome P450 (CYP) gene transfer sensitizes tumor xenografts to anticancer prodrugs such as cyclophosphamide (CPA) without a detectable increase in host toxicity. Optimal prodrug activation is achieved when a suitable P450 gene (e.g., human *CYP2B6*) is delivered in combination with NADPH-cytochrome P450 reductase (*P450R*), which encodes the flavoenzyme P450 reductase. We sought to improve this gene therapy by coordinated delivery and expression of P450 and P450R on a single bicistronic vector using an internal ribosomal entry site (IRES) sequence. Retrovirus encoding a *CYP2B6*-IRES-*P450R* expression cassette was shown to induce strong P450-dependent CPA cytotoxicity in a population of infected 9L gliosarcoma cells. Adeno-P450, a replication-defective, E1/E3 region-deleted adenovirus engineered to express *CYP2B6*-IRES-*P450R*, induced intracellular CPA 4-hydroxylation, and CPA cytotoxicity, in a broad range of human cancer cell lines. However, limited Adeno-P450 gene transfer and CPA chemosensitization was seen with certain human tumor cells, notably PC-3 prostate and HT-29 colon cancer cells. Remarkable improvements could be obtained by coinfecting the tumor cells with Adeno-P450 in combination with Onyx-017, an E1b-55k gene-deleted adenovirus that selectively replicates in p53 pathway-deficient cells. Substantial increases in gene expression were observed during the early stages of viral infection, reflecting an apparent coamplification of the Adeno-P450 genome, followed by enhanced viral spread at later stages, as demonstrated in cultured tumor cells, and in A549 and PC-3 solid tumor xenografts grown in *scid* mice. This combination of the replication-defective Adeno-P450 with a replication-conditional and tumor cell-targeted helper adenovirus dramatically improved the low gene transfer observed with some human tumor cell lines and correspondingly increased tumor cell-catalyzed CPA 4-hydroxylation, CPA cytotoxicity, and *in vivo* antitumor activity in a PC-3 tumor xenograft model. The use of tumor-selective, replicating adenovirus to promote the spread of replication-defective gene therapy vectors, such as Adeno-P450, substantially increases the therapeutic potential of adenoviral delivery systems, and should lead to increased activity and enhanced tumor selectivity of cytochrome P450 and other gene-directed enzyme prodrug therapies.

INTRODUCTION

Gene-directed enzyme prodrug therapy (GDEPT) is designed to sensitize tumor cells to cancer chemotherapeutic prodrugs. Many GDEPT strategies have been introduced over the last several years; however, only a few have advanced to the stage of human clinical trials (1–3). The success of prodrug activation gene therapy is influenced by multiple factors, including the activity and specificity of the prodrug activating enzyme, the efficiency and selectivity of gene transfer, the potency of the activated prodrug, and the strength of the bystander effect. One emerging GDEPT strategy utilizes cytochrome P450 (CYP) enzymes in combination with the flavoenzyme P450R to activate established anticancer prodrugs with demonstrated clinical utility, such as cyclophosphamide (CPA) and its isomer ifosfamide (IFA; Refs. 4, 5; reviewed in Refs. 6, 7). CPA and IFA are alkylating

agent prodrugs that induce DNA cross-linking in a cell cycle-independent manner, and ultimately trigger a mitochondrial pathway apoptotic cell death in the case of CPA (8) and either apoptosis or necrosis in the case of IFA (8, 9). CPA and IFA are activated by a subset of liver-expressed P450 enzymes (10, 11), which catalyze a 4-hydroxylation reaction that yields cell membrane-permeable, cytotoxic metabolites. These metabolites are transported from the liver to tumor cells and also normal host tissues, where they induce deleterious side effects that limit therapeutic effectiveness (12, 13).

The anticancer activity of CPA in cultured tumor cells, and in rodent and human xenograft models is substantially increased by introduction of cDNAs encoding the P450 enzymes CYP2B1 and CYP2B6, which are major catalysts of CPA activation in rat and human liver, respectively (14–17). The efficacy of this P450 GDEPT strategy may be additionally enhanced in several ways: (a) by using P450/P450R-activated bioreductive drugs that target hypoxic regions of solid tumors, either alone or in combination with CPA (18, 19); (b) by increasing the tumor/liver partition of P450 prodrugs, using thyroid hormone antagonists to suppress liver P450R expression and thereby decrease liver P450 metabolic activity (20); and (c) by administration of CPA in frequent, low doses (21) using a metronomic schedule associated with antiangiogenic activity (22).

In the present study we sought to enhance the efficiency of P450 gene delivery and P450 prodrug activation. We report improved P450 prodrug activity using an internal ribosome entry site (IRES) sequence (23) to achieve coordinate expression of P450 and P450R. We additionally show that a replication-defective adenovirus armed with a *CYP2B6*-IRES-*P450R* expression cassette (Adeno-P450) can sensitize human tumor cells of diverse tissue origin to CPA. Finally, we demonstrate that a tumor cell-targeted, conditionally-replicating E1b-55k-deleted adenovirus, closely related to the Onyx-015 oncolytic adenovirus now in Phase II/Phase III clinical trials (24–26), can be used as a helper virus to greatly increase the efficiency of tumor cell expression and spread of Adeno-P450. This effect is demonstrated both in cell culture and *in vivo* in a human xenograft model, and is shown to enhance production of cytotoxic, P450-activated CPA metabolites and thereby significantly increase tumor cell kill.

MATERIALS AND METHODS

Chemicals. CPA, chloroquine, fetal bovine serum (FBS), and puromycin were purchased from Sigma Chemical Co. (St. Louis, MO). 4OOH-CPA and 4OOH-IFA, chemically activated derivatives of CPA and IFA, respectively, were obtained from Asta Pharma (Bielefeld, Germany).

Retroviral Plasmid Construction. The retroviral plasmids pBabe-puro and pWzl-bleo are based on the pBabe series (27), and encode puromycin and bleomycin resistance genes, respectively, both being transcribed from the 3'-long terminal repeat of the viral vector. Human P450R cDNA cloned into the *EcoRI* site of pUV1 (28), obtained from Dr. Frank Gonzalez (National Cancer Institute, Bethesda, MD), was excised with *EcoRI*, and then blunt ended and subcloned into the blunt-ended *SnaBI* and *SallI* sites of pBabe-puro to yield pBabe-P450R-puro. The presence of the correct ATG initiation codon in the cloned P450R cDNA was verified by DNA sequencing. To construct pBabe-2B6-IRES-P450R-puro, the IRES sequence of pWzl-bleo was excised using *BglIII* and *NcoI*, blunt ended, and then recloned into the *SnaBI* site of pWzl-bleo to yield a pWzl-bleo derivative with two IRES sequences in tandem. The first IRES sequence was removed using *BamHI* and *BglIII*, and

Received 6/18/03; revised 10/17/03; accepted 10/24/03.

Grant support: Supported by NIH Grant CA49248 (to D. J. W.).

The costs of publication of this article were defrayed in part by the payment of page charges. This article must therefore be hereby marked *advertisement* in accordance with 18 U.S.C. Section 1734 solely to indicate this fact.

Requests for reprints: David J. Waxman, Department of Biology, Boston University, 5 Cummington Street, Boston, MA 02215. Fax: (617) 353-7404; E-mail: djw@bu.edu.

subcloned into the *Bam*HI site of pBabe-P450R-puro. The resulting plasmid, pBabe-IRES-P450R-puro, was linearized by digestion with *Spe*I and *Eco*RI, blunt ended, and then ligated to a blunt-ended *Spe*I-*Sph*I fragment encompassing the open reading frame of CYP2B6 excised from pBabe-2B6-puro (15). The resulting construct is designated pBabe-2B6-IRES-P450R-puro. The CYP2B6 cDNA used in these studies (GenBank accession no. M29874) corresponds to the wild-type (CYP2B6*) allele (29), *i.e.*, Arg22/Lys139/Gln172/Ser259/Lys262/Arg487. CYP2C18 cDNA was cut from pBabe-2C18-Met-puro (15) using *Spe*I and *Vsp*I, blunt ended, and then subcloned into *Spe*I- and *Eco*RI-linearized and blunt-ended pBabe-IRES-P450R-puro. CYP2C19 cDNA was cut from pBabe-2C19-puro (15) using *Spe*I and *Bgl*III, followed by blunt-end subcloning into the *Spe*I and *Eco*RI sites of pBabe-IRES-P450R-puro.

9L Cell Lines Coexpressing P450 and P450R cDNAs. Transfection of the ecotropic packaging cell line Bosc 23 (30) with pBabe-2B6-IRES-P450R-puro, pBabe-2C18-IRES-P450R-puro, pBabe-2C19-IRES-P450R-puro, pBabe-P450R-puro, and pBabe-IRES-P450R-puro retroviral plasmids, harvesting of retroviral supernatants, and infection of rat 9L gliosarcoma cells were carried out as described (15), with the following modifications. Bosc 23 cells were plated at 2.5×10^6 cells in a 60-mm dish. Fresh media (4 ml) containing chloroquine (25 μ M) was added to the cells 16 h later. The cells were cotransfected 1 h later with 5 μ g of retroviral plasmid DNA and 2.5 μ g of the helper plasmid pKat (31) using 9 μ l of the cationic liposome Fugene 6 (Boehringer-Mannheim) in a total volume of 40 μ l DMEM without FBS. Pools of cells resistant to puromycin (2.5 μ g/ml) were selected 48 h later over a 2–3-day period as described (15). Drug-resistant pools of cells were propagated and then assayed for P450R-catalyzed, NADPH-dependent cytochrome C reduction (A_{550} measured at 30°C) in isolated microsomes (15). A 3–4-fold increase in P450R activity was exhibited by the 9L/pBabe-IRES-P450R cells *versus* a 2–3-fold increase in the pools of 9L/P450-IRES-P450R transfectants.

Growth Inhibition Assay. The chemosensitivity of P450-expressing 9L cell lines was determined using a 4-day growth inhibition assay, with cells plated in triplicate at 4000 cells/well of a 48-well plate 1 day before treatment with CPA continuously for 4 days (15). The same assay was used to evaluate the intrinsic sensitivity of tumor cells to the chemically activated CPA and IFA derivatives 4OOH-CPA and 4OOH-IFA (0–5 μ M). Cells remaining at the end of 4 days were stained and quantified using a crystal violet/alcohol-extraction assay (15). Data are expressed as cell number (A_{595}) relative to drug-free controls, mean \pm SD values for triplicate samples, unless indicated otherwise.

Construction of Recombinant Adenovirus. A replication-defective, E1 and E3 region-deleted adenovirus encoding CYP2B6 and P450R, designated Adeno-P450, was constructed using the AdenoX expression system (Clontech Laboratories Inc., Palo Alto, CA). pBabe-2B6-IRES-P450R-puro was linearized using *Bam*HI, blunt ended, and the CYP2B6-IRES-P450R cassette then cut with *Dra*I and ligated into the *Dra*I site of pShuttle (Clontech Labs). The resulting plasmid, pShuttle-2B6-IRES-P450R, was used to construct the recombinant adenovirus, Adeno-P450, as described in the manufacturer's kit. The cytomegalovirus-IE promoter of pShuttle drives Adeno-P450-directed expression of CYP2B6 and P450R, and ensures robust expression in a wide range of cell lines and tissues. The conditional replicating virus Onyx-017, which contains wild-type viral E3 region and an E1b-55k gene deletion equivalent to that of Onyx-015 (25), was obtained from Onyx Pharmaceuticals, Inc. (Richmond, CA). Adeno- β -galactosidase (Adeno- β Gal) is an E1- and E3-region deleted, replication-deficient adenovirus that contains a β -galactosidase reporter under the control of a cytomegalovirus promoter and was used in our previous studies (14).

Adenovirus Purification. Adenoviral stocks were propagated in human kidney 293 cells grown in 100-mm plates at 37°C in a humidified, 5% CO₂ atmosphere in high glucose DMEM containing 10% FBS. Cells were grown to ~90% confluence and then infected with Adeno-P450 at a multiplicity of infection (MOI) of ~5 viral particles per cell. Alternatively, 3–5 ml of –80°C frozen culture supernatant obtained from Adeno-P450-infected 293 cells was used to reinfect the 293 cells. Seventy-two h after infection, >80–90% of the cells became rounded, and 10–20% of the cells were floating. The cells were then collected by centrifugation and resuspended in 20 ml of buffer A [10 mM Tris-base (pH 8.0) and 1 mM MgCl₂]. The virus was released by three freeze-thaw cycles, alternating between an alcohol-dry ice bath and a 37°C bath. The cell lysate was centrifuged at 4°C for 10 min at 3,000 rpm, and the supernatant was placed on ice. The residual cell pellet was re-extracted in the same manner with 10 ml of buffer A, and the combined supernatants were treated

with Benzonase (0.5–1 units/ml) at room temperature for 30 min. The treated suspension was layered carefully onto a cold CsCl step gradient comprised of 10 ml of light CsCl [1.20 g/ml: 22.39 g CsCl + 77.6 ml of 10 mM Tris-base (pH 8.0)] layered on top of 10 ml of heavy CsCl [1.45 g/ml: 42.2 g CsCl + 57.8 ml of 10 mM Tris-base (pH 8.0)]. Samples were centrifuged in a Sorval Pro ultracentrifuge in an SW28 rotor at 4°C for 2 h at 20,000 rpm. The banded virus was collected and diluted with an equal volume of 10 mM Tris-base (pH 8.0), and rebanded on a second CsCl step gradient consisting of 4 ml each of light CsCl and heavy CsCl as described above, then centrifuged overnight at 4°C at 20,000 rpm in a Sorval SW41Ti rotor. The purified virus was desalted by dialysis against 10 mM Tris-base (pH 8.0), 1 mM MgCl₂, and 10% glycerol, with the effectiveness of desalting verified by conductivity measurement. Alternatively, the purified virus was passed through a Bio-Rad Econo-Pac 10DG Column pre-equilibrated with 30 ml of column buffer [10 mM Tris-base (pH 8.0), 1 mM MgCl₂, and 10% glycerol]. The virus suspension was loaded onto the column, and samples were collected immediately after the first 2.5-ml eluent. Viral titers were quantitated using the Adeno-X Rapid Titer kit (Clontech Labs), as described in the manufacturer's kit. Virus aliquots were stored at –80°C.

Adenoviral Infection of Human Tumor Cell Lines and CPA Cytotoxicity Assays. Thirteen human tumor cell lines selected from the NCI-60 panel (see Fig. 2, below; Ref. 32) were obtained from Dr. Dominic Scudiero (National Cancer Institute). The A549 lung cancer cell line was also obtained from Onyx Pharmaceuticals, Inc. and was used in all of the helper adenovirus experiments. In the experiments shown in Fig. 2 (see below), cells were seeded in six-well plates at 75,000 cells per well. Sixteen h later the cells were infected for 1 h with Adeno-P450 at an MOI of 90 plaque-forming units (pfu)/cell in 1 ml of RPMI 1640 containing 5% FBS, after which the medium was removed and replaced with fresh medium. Cells were incubated for an additional 48 h and cell lysate then prepared by sonication. P450R activity in 20 μ g cell lysate was assayed to obtain an overall indication of viral transduction efficiency. In other experiments (Fig. 3B; below), human tumor cells were plated in triplicate at 8,000 cells/well of a 24-well plate 18–24 h before adenovirus infection. Cells were infected for 1 h with Adeno- β Gal at MOI 50 or with Adeno-P450 at MOI values of 25, 65, and 125 pfu/cell in DMEM containing 5% FBS. Fresh medium (1 ml) was then added to each well, followed by an additional 24-h incubation. The cells were then treated with CPA (0–1 mM, as specified in each experiment) and cultured up to 4 days. Cells remaining at the end of the experiment were stained with crystal violet and quantified (A_{595}) as percentage of survival relative to untreated cells.

Onyx-017 Helper Virus Experiments. In a typical experiment, A549 cells were plated in six-well plates at 75,000 cells/well. Cells were infected for 1 h with Adeno- β Gal or Adeno-P450, either alone or in combination with Onyx-017, at MOIs specified in each experiment. The medium was then replaced with virus-free medium. Individual plates of cells were stained with 5-bromo-4-chloro-3-indolyl- β -D-galactopyranoside (X-gal) 1–5 days later to evaluate the spread of Adeno- β Gal. β -Galactosidase activity was quantitated using a microtiter plate reader (A_{650}) after resuspending the X-gal stain in 1 ml DMSO/well of a six-well plate (18). To determine whether the infected cells continue to release infective Adeno- β Gal viral particles, the supernatant from day 4- or day 5-infected cells was used to infect fresh A549 cells, which were stained with X-gal 48 h later.

In other experiments, the effect of Onyx-017 on Adeno-P450-dependent CYP2B6 expression and CYP2B6-catalyzed 4-hydroxy-cyclophosphamide (4OH-CPA) production was assayed, as follows. Twenty-four h after infection with adenovirus, the cells were treated with 1 mM CPA in 3 ml of fresh RPMI 1640 containing 5% FBS and 0.5 mM semicarbazide to stabilize the 4OH-CPA metabolite. After 5 h of CPA treatment, 0.5 ml of culture supernatant was removed and assayed for the presence of 4OH-CPA released into the culture medium (33). The cells were then washed once with PBS, scraped from the wells, and lysed by sonication in 50 mM potassium phosphate buffer and 1 mM EDTA (pH 7.4) containing 20% glycerol. The procedure was repeated on days 2–4 after viral infection in parallel sets of plates. Western blot analysis of CYP2B6 protein (30 μ g sonicated cell lysate protein/well) was performed using mouse anti-CYP2B6 monoclonal antibody and lymphoblast-expressed CYP2B6 protein (0.6–1 pmol/lane) as standard (BD-Gentest, Inc., Woburn, MA).

To assess the impact of Onyx-017 on Adeno-P450-mediated CPA cytotoxicity, human tumor cell lines U251, PC-3, and A549 were plated in 24-well plates at 14,000 cells/well and infected 24 h later with Adeno-P450 (A549 and

PC-3, MOI 12; U251 cells, MOI 3), either alone or in combination with Onyx-017 (MOIs 0, 0.3, 1, 2, 3, and 4). Virus was incubated with the cells for 3.5 h in RPMI 1640 medium (0.2 ml/well), after which an additional 1 ml of fresh RPMI 1640 was added to each well. The medium was removed 24 h later and 1 ml of fresh medium containing CPA (0, 0.25, 0.5, and 1 mM) was added to the cells. After 2 days of CPA treatment, the medium was replaced with 1 ml of fresh CPA-containing medium for an additional 5 days, after which cell survival was assayed by crystal violet staining.

Visualization of Helper Virus Dynamics by Immunocytochemistry. Confocal immunofluorescence microscopy was used to assay the expression of CYP2B6 in A549 cells infected with Adeno-P450 (MOI 25) or infected with Adeno-P450 (MOI 5) in combination with Onyx-017 (MOIs 0.1, 0.5, and 5). A549 cells (4000 cells/well) were plated in an eight-well LAB-TEK Chamber Slides (Nalgen Nunc, International). Cells were infected with adenovirus for 1 h at the indicated MOIs, after which the medium was replaced with 0.2 ml of fresh RPMI 1640 containing 5% FBS. Cells were then cultured for an additional 48 h. CYP2B6 immunostaining was then carried out as follows. Cells were washed with PBS buffer and fixed in 100% methanol at room temperature for 10 min. Samples were air-dried and then incubated twice for 10 min in PBS containing 3% FCS for blocking. Monoclonal anti-CYP2B6 antibody diluted 1/1000 into PBS containing 3% FCS (50 μ l) was then added to each well. The plates were covered with aluminum foil and incubated for 1 h at 37°C in a tissue culture incubator. Cells were washed twice for 5 min with 100 μ l of 3% FCS in PBS and then incubated with FITC-conjugated antimouse antibody (Molecular Probes, Inc., Eugene, OR) diluted 1:1000 in 3% FCS in PBS and incubated for 1 h at 37°C. Cells were washed under dim light with 3%

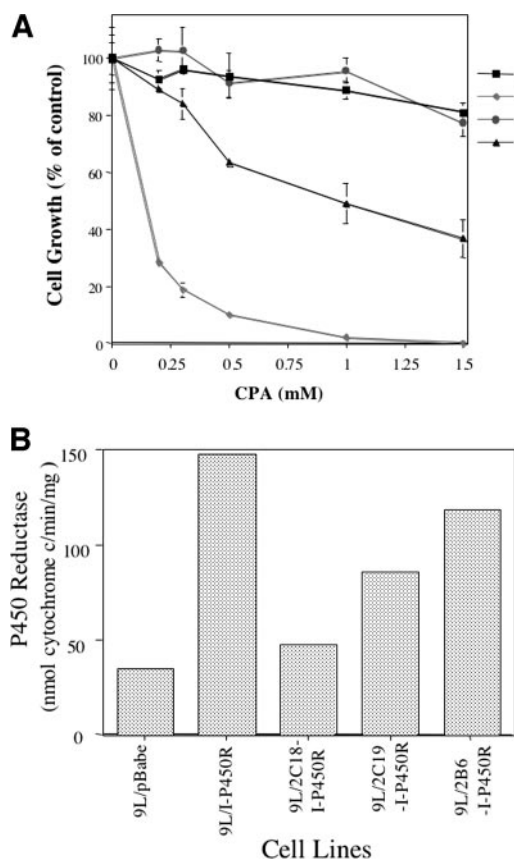


Fig. 1. Chemosensitivity of 9L gliosarcoma cells transduced with retroviral P450-internal ribosome entry site (IRES)-NADPH-cytochrome P450 reductase (P450R) bicistronic constructs. Cells were seeded at 4000 cells/well in 48-well plates and treated with increasing concentrations of cyclophosphamide (CPA; 0–1.5 mM) for 4 days as described in “Materials and Methods.” A, growth inhibition assay carried out with each of the indicated 9L/P450-IRES-P450R cells, and 9L/pBabe (control) cells. Cell growth in comparison to drug-free controls was determined by crystal violet staining. Data are presented as mean values for $n = 3$ replicates; bars, \pm SD. B, P450R enzyme activities (rate of cytochrome C reduction) determined in assays of microsomes (20 μ g protein) isolated from 9L/pBabe, 9L/IRES-P450R (9L/I-P450R), and each of the indicated 9L/P450-IRES-P450R cell lines.

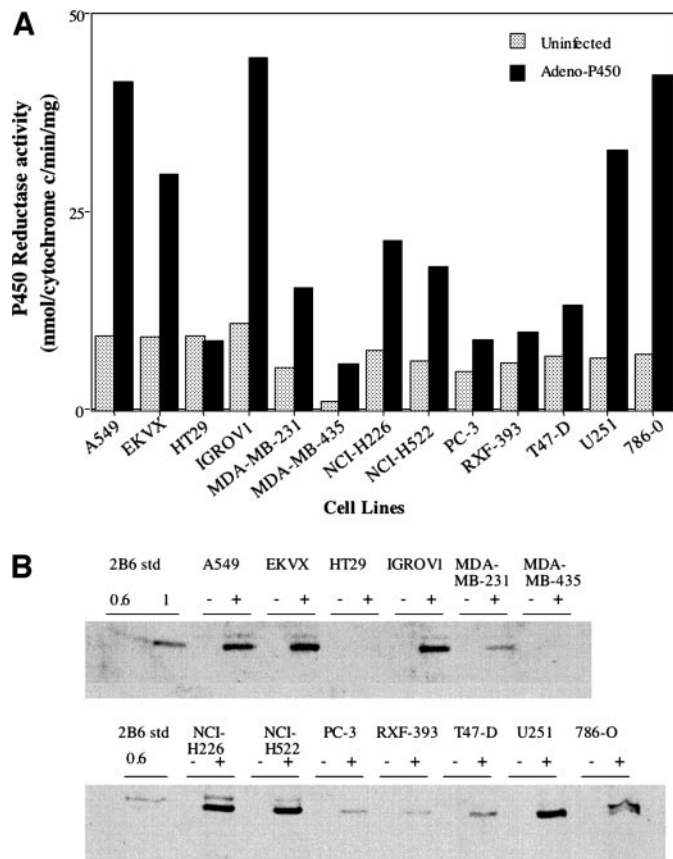


Fig. 2. Expression of NADPH-cytochrome P450 reductase (P450R) and CYP2B6 in panel of human tumor cell lines infected with Adeno-P450. Cells were seeded in six-well plates at 75,000 cells per well. Sixteen h later the cells were uninfected (–) or were infected with Adeno-P450 (+) at multiplicity of infection (MOI) 90 for 1 h as described in “Materials and Methods.” Cell lysates were prepared 2 days later. A, expression of P450R in each cell line as measured by cytochrome C reduction (representative set of assays using 20 μ g cell lysate protein). B, Western blots analyzing the same set of cell lysates for CYP2B6 protein (30 μ g protein/well) using mouse anti-CYP2B6 monoclonal antibody and lymphoblast-expressed CYP2B6 as standard (0.6 and 1 pmol; left lanes of each gel).

FCS in PBS. To visualize cell nuclei, 50 μ l of propidium iodide (5 ng/ml in PBS) was added to the cells for 5 min, followed by two PBS washes. Slides were treated with a drop of Fluoroguard anti-fade reagent (Bio-Rad), covered with a coverslip sealed with nail polish and stored at -20°C before confocal microscopy. Cells were scanned with a BX-50 confocal laser-scanning microscope (Olympus Corp., New Hyde Park, NY) equipped with $\times 60$ objective (Carl Zeiss, Thornwood, NY) and photographed.

Adeno-P450 Spread in A549 and PC-3 Xenografts in Scid Mice. Seven-week-old (25–29 g) male ICR/Fox Chase mice, an outbred *scid* immunodeficient strain (Taconic Farms, Germantown, NY), were injected s.c. at each posterior flank with 4×10^6 A549 or PC-3 tumor cells in a volume of 0.5 ml of serum-free DMEM using a 0.5-inch, 29-gauge needle and a 1-ml insulin syringe. Tumor sizes were measured twice a week using external calipers. Tumors reaching approximately 200–300 mm^3 in size were injected with Adeno-P450, alone or in combination with Onyx-017, using an established protocol (intratumoral injection of 50 μ l containing 5×10^7 pfu of each virus, daily for 5 days). Tumors were excised on day 2, 7, and 14 after the last virus injection. The efficiency of Adeno-P450 gene delivery was monitored by immunofluorescence analysis of cryosectioned tumor slices using anti-CYP2B6 antibody. Mice were killed by cervical dislocation, tumors were excised and frozen in dry ice-cooled isopentane for 3 min, and were sectioned with a cryostat to give 25 μ m sections. Sections were fixed immediately in -10°C acetone and processed for immunohistochemical analysis as described above. Tumor extracts from PC-3 tumors were prepared by homogenization in 50 mM KPi buffer and 1 mM EDTA (pH 7.4) containing 20% glycerol. To assess the Onyx helper virus effect *in vivo*, 30 μ g of cell lysate was analyzed by Western blotting using anti-2B6 mouse monoclonal antibody.

PC-3 Xenograft Growth Delay Studies in Scid Mice. PC-3 prostate tumors were implanted s.c. at each posterior flank in 8-week-old male *scid* mice (25–29 g) as described above. Adeno-P450 and/or Onyx-017 was injected intratumorally using the viral doses and 5-day injection schedule described above, beginning 28 days after tumor implantation. Mice were treated with CPA using a metronomic schedule used in our earlier studies of 9L/P450 tumors in the same *scid* mouse model (21): 140 mg CPA/kg body weight every 6 days beginning 5 days after the last adenovirus injection (*i.e.*, day 37 after tumor implantation). Mice were divided into five treatment groups, each containing 5–7 tumors: (a) untreated; (b) CPA-treated; (c) Adeno-P450-injected and CPA-treated; (d) Onyx-017-injected and CPA-treated; and (e) Adeno-P450 and Onyx-017 coinjected and CPA-treated. Tumor areas (length \times width) were measured twice a week using vernier calipers (Manostat Corp., Zurich, Switzerland), and tumor volumes were calculated based on: $\text{vol} = \pi/6 (\text{length} \times \text{width})^2$. The effect of CPA on tumor growth rate was calculated relative to the tumor volume on day 35 (*i.e.*, 2 days before the first CPA injection). This approach allows for comparisons of the effects of drug treatment on the growth of tumors that differ in size at the time of initial drug treatment. One-way ANOVA analysis using the Bonferroni multiple comparison test was carried out using GraphPad Prism 4 software (San Diego, CA).

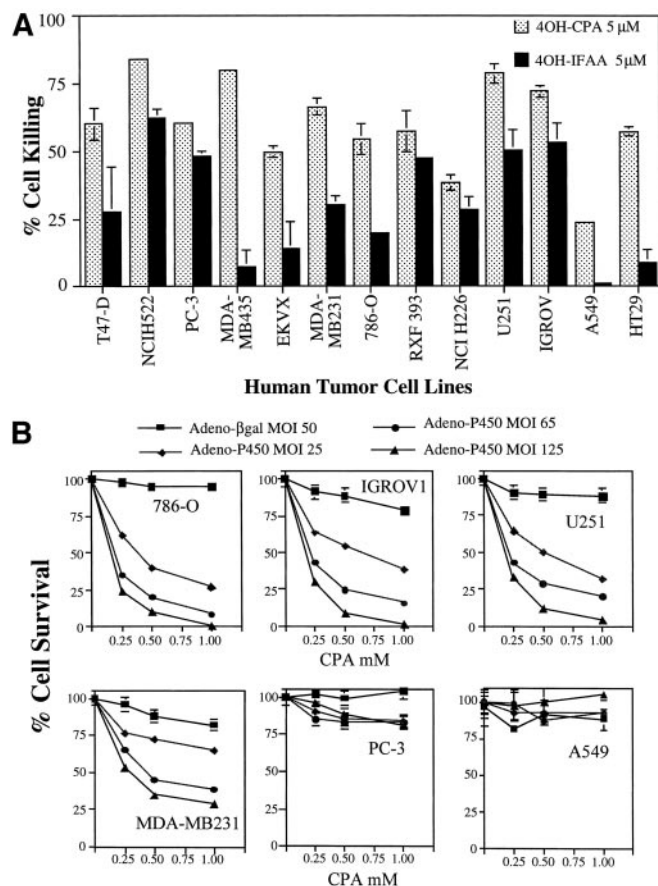


Fig. 3. Chemosensitivity of human tumor cell line panel to cyclophosphamide (CPA) and ifosfamide (IFA). **A**, each cell line was treated with 5 μM 4OH-CPA or 4OH-IFA for 4 days. Cells remaining at the end of the experiment were quantified by crystal violet staining. Data are expressed as percentage growth inhibition compared to the untreated cell controls, mean for triplicate samples; *bars*, \pm SD. Similar profiles were evident in parallel experiments using 1, 2, and 3 μM of each drug. *Error bars* not shown are too small to be seen. **B**, sensitization of the six indicated cell lines to CPA after Adeno-P450 infection. Cells were plated in triplicate at 8000 cells/well of a 24-well plate 18–24 h before adenovirus infection. Cells were then infected for 1 h with Adeno- β Gal at multiplicity of infection (MOI) 50 or with Adeno-P450 at MOIs of 25, 65, and 125 in DMEM containing 5% FBS. Fresh medium (1 ml) was then added to the wells followed by an additional 24-h incubation. Cells were then treated with CPA (0–1 mM). Cells remaining after 4 days of growth were quantified by crystal violet staining as described in “Materials and Methods.”

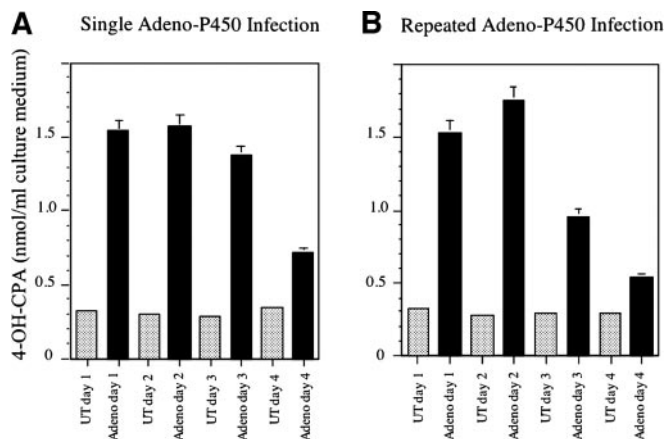


Fig. 4. 4-Hydroxy-cyclophosphamide production in Adeno-P450-infected U251 cells. Cells were plated in six-well plates at 75,000 cell/well and infected with Adeno-P450 for 1 h, after which the medium was replaced as described in “Materials and Methods.” Beginning 24 h after infection (= day 1) and on days 2, 3, and 4 thereafter, plates of cells were assayed for cyclophosphamide (CPA) 4-hydroxylase activity using 1 mM CPA and a 5-h incubation period, as described in “Materials and Methods.” Cells were infected on day 0 with Adeno-P450 at multiplicity of infection (MOI) 65 (**A**) or were infected with Adeno-P450 repeatedly on days 0, 1, 2, and 3 at a daily dose of MOI 65 (**B**).

RESULTS

Coordinate Expression of P450 and P450R Linked by IRES Sequence. Retroviral vectors based on the pBabe-puro series (27) were used to construct recombinant retroviruses incorporating human *CYP2B6*, *CYP2C18*, and *CYP2C19* in bicistronic constructs linked in tandem with human *P450R* via an IRES sequence. Rat 9L gliosarcoma cells were infected with each retrovirus to assess the functionality of each bicistronic construct. Pools of stably infected cells were obtained and characterized in comparison with a control retroviral cell line, 9L/pBabe. Fig. 1A shows that the bicistronic construct *CYP2B6*-IRES-*P450R* sensitized the pool of infected 9L cells to CPA to an extent far greater than the two other bicistronic retroviral constructs under the same conditions. *CYP2C19*-IRES-*P450R* retrovirus sensitized 9L cells to CPA only at higher doses of the prodrug, consistent with the lower intrinsic CPA 4-hydroxylase activity of *CYP2C19* compared with *CYP2B6* (34), whereas the *CYP2C18*-IRES-*P450R* retrovirus was ineffective (Fig. 1A).

P450R activity was increased in 9L cells infected with *CYP2B6*-IRES-*P450R* or *CYP2C19*-IRES-*P450R* retrovirus, as assayed in extracts prepared from virus-infected cells. *P450R* activity was somewhat higher in 9L/IRES-*P450R* cells, which were established by infection with the single cistron retroviral construct IRES-*P450R* (Fig. 1B). This finding is consistent with reports showing reduced expression of a second cistron following an IRES sequence (35). Most notable was the very low *P450R* activity of 9L/2C18-IRES-*P450R* cells, which approached the background activity of 9L/pBabe controls. This finding is reminiscent of the very low level of retroviral expression of *CYP2C18* seen in our earlier study (15). Additional characterization of the *CYP2C18* cDNA in a series of *CYP2C18*-IRES-*P450R* retroviral infection experiments using the *P450R* cistron as a reporter gene revealed that the bicistronic construct was destabilized by sequences between *CYP2C18* cDNA nucleotides 1471 and 1751, which includes 40 nucleotides at the 3' end of the open reading frame of *CYP2C18* (data not shown).

Adenoviral Expression of *CYP2B6*-IRES-*P450R* in Human Tumor Cell Lines. A replication-defective, E1- and E3-region-deleted adenovirus containing the *CYP2B6*-IRES-*P450R* expression cassette was engineered and designated Adeno-P450. The ability of this virus to induce *P450* and *P450R* expression was evaluated in a panel of 13

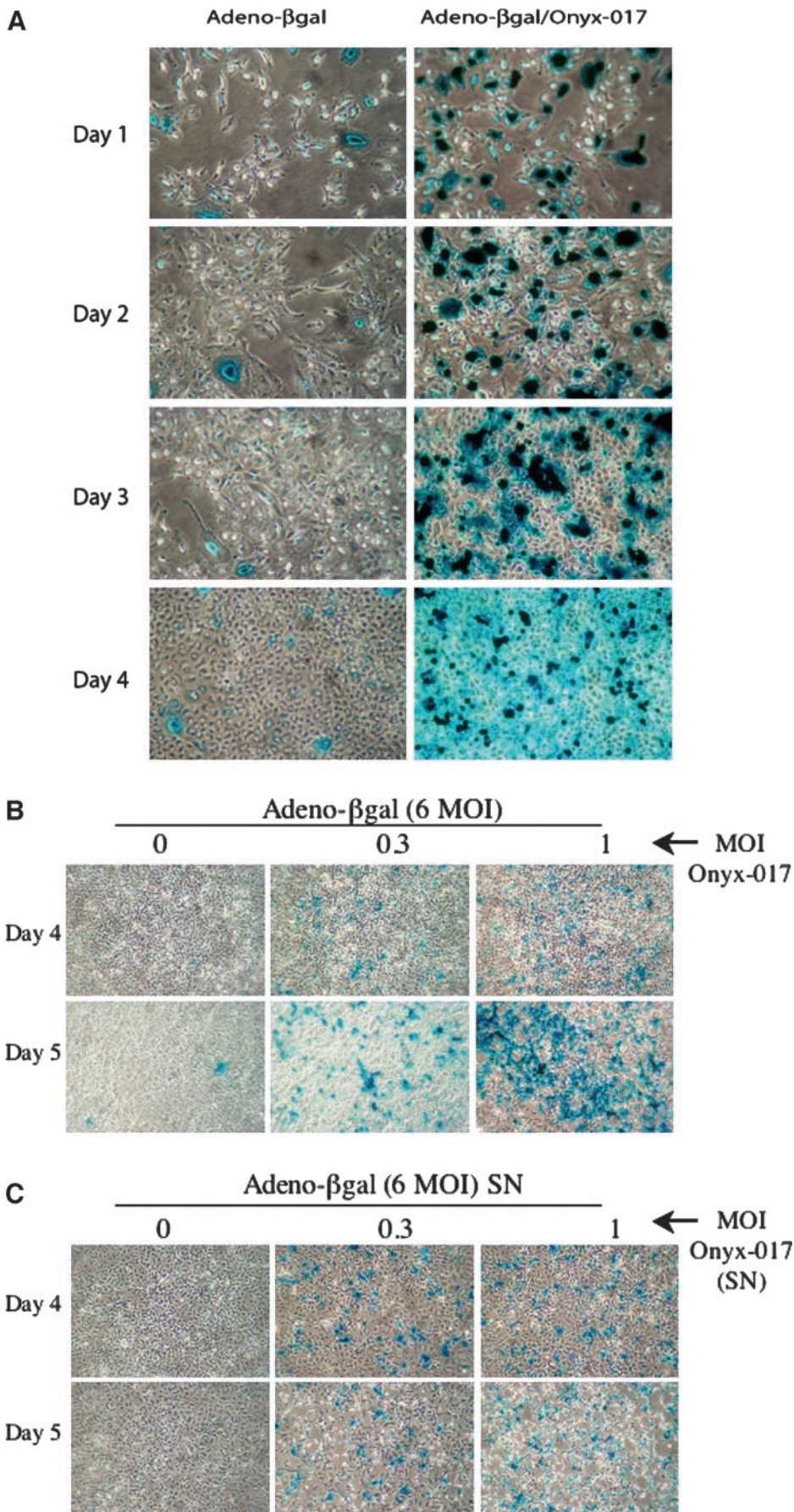


Fig. 5. Helper effect of Onyx-017 toward Adeno- β Gal (A–C) and Adeno-P450 (D). A, A549 cells plated in six-well plates at 75,000 cells/well were infected for 1 h with Adeno- β Gal [multiplicity of infection (MOI) 25] alone or in combination with Onyx-017 (MOI 5). Shown are cells stained with 5-bromo-4-chloro-3-indolyl- β -D-galactopyranoside (X-gal) to monitor the expression of Adeno- β Gal on days 1, 2, 3, and 4 after infection in the absence (*left set of panels*) or presence (*right set of panels*) of Onyx-017. B, A549 cells plated in 12-well plates at 30,000 cells/well were infected for 1 h with Adeno- β Gal (MOI 6) alone or in combination with Onyx-017 (MOI 0.3 or 1). Shown are the X-gal stained cells on days 4 and 5 postinfection at the indicated Onyx-017 MOIs. C, Supernatant (SN) from the day 4- and day 5-infected cells in B were used to infect fresh A549 cells, which were stained with X-gal 48 h after infection. X-gal staining is only seen in cells infected with supernatant from the Onyx-017-coinfected cultures and is indicative of the presence of viable Adeno- β Gal particles in the supernatant. D, A549 cells were infected for 1 h with Adeno-P450 alone (MOI 25) or with Adeno-P450 (MOI 5) in combination with Onyx-017 (MOIs 0.1, 0.5, and 5, as indicated). Cells were cultured for an additional 48 h and then were stained using monoclonal antibody to CYP2B6 (*left set of panels*). Cell nuclei were visualized by staining with propidium iodide (*right set of panels*).

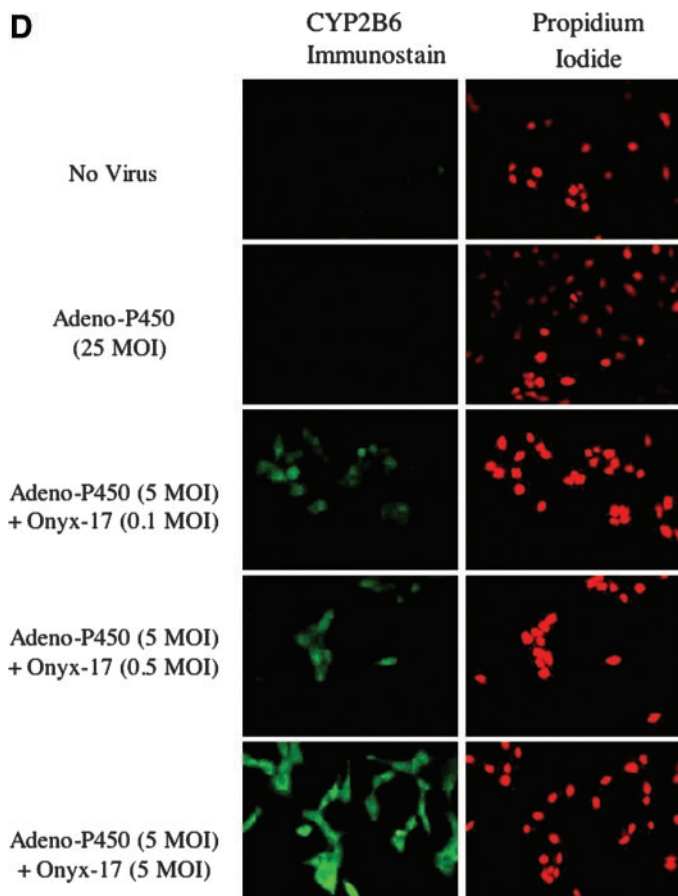


Fig. 5. Continued.

cell human tumor lines that represents the broad range of tumor tissue types included in the full NCI-60 panel (Ref. 32; Fig. 2). Up to a 7-fold increase in total cellular P450R expression (rate of P450R-catalyzed cytochrome C reduction) was observed. Six of the 13 cell lines showed at least a 4-fold increase in P450R activity and 9 showed at least a 2-fold increase. CYP2B6 protein was also increased significantly in 9 of the cell lines after Adeno-P450 infection (Fig. 2B). The extent of this latter increase generally correlated with the cell line-dependent increases in P450R expression (Fig. 2A), consistent with the coordinate expression of CYP2B6 and P450R linked by the IRES sequence. Little or no increase in P450R activity or CYP2B6 protein expression was detected in the four remaining cell lines. This reflects poor adenoviral infectivity and/or expression in the case of PC-3 prostate cancer and HT-29 colon carcinoma cells, as demonstrated by the weak (PC-3 cells) and extremely weak staining with the β -galactosidase substrate X-gal (HT29 cells) after infection with 50 MOI of Adeno- β Gal, which encodes β -galactosidase (data not shown). X-gal staining was intermediate in A549 cells and strongest in cell lines U251, IGROV, and 786-O, where 50–70% of the cells stained under the same conditions of Adeno- β Gal infection (data not shown). These findings may indicate substantial cell line-dependent differences in expression of the integrins and CAR proteins that serve as receptors for adenovirus and/or differences in the intrinsic strength of the cytomegalovirus promoter used to regulate the β -galactosidase reporter.

Adeno-P450 Sensitizes Human Tumor Cells to CPA. The 13 human tumor cell lines were characterized with respect to their intrinsic sensitivities to 4OOH-CPA and 4OOH-IFA, chemically activated derivatives of CPA and IFA that decompose in aqueous media

to form the active metabolites 4OH-CPA and 4OH-IFA, respectively. Growth inhibition assays demonstrated that all 13 of the cell lines were more sensitive to 4OOH-CPA than 4OOH-IFA (5 μ M; Fig. 3A), as are rat gliosarcoma 9L cells (15). These differences in intrinsic sensitivity to 4OOH-CPA versus 4OOH-IFA may reflect differences in the cellular response to drug-induced DNA damage, which involves a 5-atom cross-link in the case of phosphoramidate mustard, derived from CPA, and a 7-atom cross-link in the case of isophosphoramidate mustard, derived from IFA. A549 lung carcinoma cells were the least sensitive to both oxazaphosphorines. This finding is consistent with the expression in A549 cells of high levels of aldehyde dehydrogenase forms 1 and 3, which convert 4OH-CPA and 4OH-IFA to the corresponding inactive carboxyphosphamides (36), and would render this cell line particularly resistant to P450-activated CPA.

Next, six of the tumor cells lines were additionally investigated to determine whether Adeno-P450 infection results in a level of CYP2B6 and P450R expression that is sufficient to sensitize the cells to CPA. U251 (brain), IGROV1 (ovarian), 786-O (renal), PC-3 (prostate), MDA-MB-231 (breast), and A549 (lung) cells were infected with Adeno-P450 at MOIs of 25, 65, and 125, or with Adeno- β Gal (MOI 50) as a control (Fig. 3B). Increased CPA chemosensitivity was achieved with increasing MOI of Adeno-P450 in four of the six cell lines. The control virus, Adeno- β Gal, had no effect, demonstrating that the increase in CPA cytotoxicity is cytochrome P450-dependent. Adeno-P450 did not appreciably sensitize PC-3 cells to CPA, which likely reflects the poor intrinsic adenoviral gene transfer in these cells (Fig. 2, A and B). A549 cells were readily infected by Adeno-P450 at the high MOIs used in these experiments (Fig. 2, A and B), but were nevertheless resistant to CPA, consistent with the low intrinsic sensitivity of these cells to activated CPA (Fig. 3A).

Repeat Infection of Tumor Cells Does Not Enhance Adeno-P450 Infection or CPA Activation. Experiments were carried out in U251 cells to determine whether the expression of P450 and P450R following Adeno-P450 infection leads to sustained production of the P450-generated cytotoxic CPA metabolite 4OH-CPA. Fig. 4A shows that the capacity of U251 cells for CPA 4-hydroxylation increased rapidly and became near maximal 1 day after Adeno-P450 infection. CPA 4-hydroxylase activity was maintained for 3 days, after which the cell capacity for CPA activation declined. Repeat infection of the cells with Adeno-P450 (MOI 65 applied each 24 h) did not additionally increase the cell capacity to activate CPA (Fig. 4B) nor did it increase the level of transgene expression, as monitored by P450R activity (data not shown).

Replication-Conditional Onyx-017 Virus Promotes Amplification and Tumor Cell Spread of Adeno- β Gal and Adeno-P450. In cells infected with wild-type adenovirus, the viral E1b protein must bind to and inactivate the p53 protein of the host cell in order for the virus to initiate replication (26). However, when the viral E1b-55k gene is deleted, e.g., as in the case of the Onyx-015 adenovirus and its wild-type E3 region counterpart Onyx-017, efficient viral replication cannot proceed in cells that retain a functional, wild-type p53 pathway. Consequently, replication of the Onyx virus is largely restricted to tumor cells, which are generally deficient in p53 function (37). Given the ability of the Onyx adenovirus to spread by tumor cell lysis, we investigated whether Onyx-017 can be used as a helper virus to facilitate amplification and cell-to-cell spread of replication-defective viruses such as Adeno- β Gal and Adeno-P450. We first tested this hypothesis in A549 cells coinfecting with Adeno- β Gal (MOI 25) and Onyx-017 (MOI 5). In the absence of Onyx-17, β Gal expression was detectable in comparatively few A549 cells, as judged by staining with X-gal. Moreover, the level of transgene expression increased marginally whereas the number of infected cells remained essentially unchanged as the cell population grew over a 4-day period (Fig. 5A,

left). By contrast, when the cells were infected with Adeno- β Gal in combination with Onyx-017, the number of infected cells (Fig. 5A, right) and the overall level of β -gal activity (Fig. 6A; data shown for a range of Onyx-017 MOIs) both increased dramatically in a time-dependent manner. The strong increase in X-gal staining activity in individual cells seen early in the experiment (e.g., day 1 cells; Fig. 5A, right) is likely to reflect coamplification of the Adeno-P450 genome by the replicating Onyx virus, whereas the spread of X-gal staining to encompass a larger fraction of cells in the population by day 4 suggests that infectious Adeno- β Gal virus particles are produced and released into the supernatant, followed by secondary infection of virus-naïve cells. This conclusion was verified in a separate experiment carried out at much lower viral MOIs, where supernatant obtained from day 4 and day 5 cultures of A549 cells coinfecting with Adeno- β Gal (MOI 6) and Onyx-017 (MOIs 0.3 and 1; Fig. 5B) was used to infect a fresh plate of A549 cells. An Onyx-017-dependent increase in X-gal staining of the fresh cells was observed (Fig. 5C), supporting the proposed role of Onyx-017 in enhancing the ability of Adeno- β Gal to replicate within and spread to other tumor cells. However, as a result of the intrinsic oncolytic activity of Onyx-017, a decline in X-gal staining with time was seen in cultures infected with Onyx-017 at higher MOIs. In the case of A549 cells, this oncolytic activity was typically manifest by day 3–4 in cells infected with Onyx-017 at MOIs 5 and 10 (Fig. 6A). Comparable results were obtained at a later time point in cells infected at lower MOIs (data not shown).

The helper effect of Onyx-017 was confirmed in separate experiments using Adeno-P450. Fig. 5D shows the beneficial effect of Onyx-017 in enhancing the expression of Adeno-P450 in A549 cells, as visualized by confocal immunofluorescence staining with antibody to CYP2B6. Whereas CYP2B6 expression in Adeno-P450-infected A549 cells (MOI 25) was at background levels 48 h after infection, robust CYP2B6 expression was evident when the cells were infected with a 5-fold lower dose of Adeno-P450 (MOI 5) in combination with low levels of Onyx-017 (MOIs 0.1, 0.5, and 5). P450-dependent CPA 4-hydroxylase activity was also greatly enhanced by coinfection of Adeno-P450 with Onyx-017, with the level of prodrug activation reaching a maximum at day 4 (Fig. 6B). By contrast the CPA 4-hydroxylase activity of cells infected with Adeno-P450 alone was still at background levels at the same time point. This Onyx-017-dependent increase in A549 cell 4OH-CPA production was readily apparent at an Onyx-017 MOI as low as 0.1, despite the high level of aldehyde dehydrogenase activity present in these cells (36). Moreover, this increase was associated with a strong, Adeno-P450- and Onyx-017-dependent expression of CYP2B6 protein, as shown by Western blot analysis (Fig. 6C).

Onyx-017 Enhances Adeno-P450-Mediated CPA Cytotoxicity.

To additionally establish the utility of the Onyx-017 helper system in the context of P450-based GDEPT, cytotoxicity experiments were carried out using three human tumor cell lines: U251 cells, which are intrinsically sensitive to 4OH-CPA cytotoxicity (Fig. 3A); A549 cells, which are intrinsically resistant to 4OH-CPA (Fig. 3A); and PC-3 cells, which are resistant to adenoviral infection (Fig. 2) but intrinsically sensitive to 4OH-CPA (Fig. 3A). Cells were infected with Adeno-P450 (MOI 12 for PC-3 and A549 cells; MOI 3 for U251 cells) either alone or in combination with Onyx-017 (MOIs ranging from 0 to 4). Cells were treated with CPA beginning 24 h after infection, and cell survival was assayed 7 days later (Fig. 7). In the case of U251 cells, which become sensitized to CPA when Adeno-P450 is delivered at high viral titers (MOIs ranging from 25 to 125; Fig. 3B) but not at low titers (i.e., MOI 3), Onyx-017 strongly increased Adeno-P450-dependent CPA cytotoxicity (Fig. 7A). A major increase in CPA toxicity was also seen after coinfection of the Adeno-P450-resistant

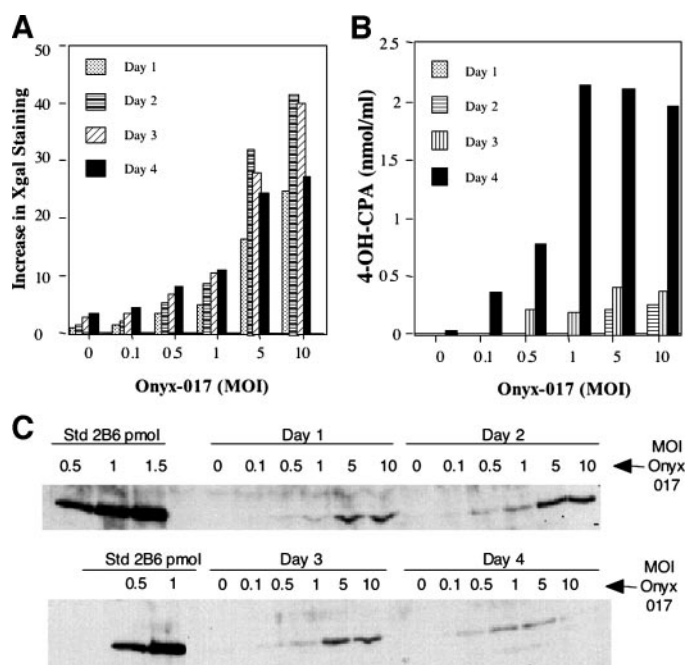


Fig. 6. Assay of Onyx-017 helper virus activity. A, A549 cells were grown and treated with Adeno- β Gal alone or in combination with Onyx-017 [0–10 multiplicity of infection (MOI), as indicated] as described in Fig. 5A. Data shown are X-gal (5-bromo-4-chloro-3-indolyl- β -D-galactopyranoside) staining intensities (A_{620}), determined after resuspending the dye in 1 ml DMSO/well of a six-well plate, and expressed as fold-increase compared to day 1 cells infected with Adeno- β Gal in the absence of Onyx-017. B, A549 cells (75,000 cells/well of a six-well plate) were infected for 1 h with Adeno-P450 (MOI 25) or with Adeno-P450 (MOI 5) in combination with Onyx-017 (MOIs 0.1, 0.5, 1, 5, and 10). 4-Hydroxy-cyclophosphamide production over a 5-h incubation period was assayed in parallel sets of plates analyzed on days 1, 2, 3, and 4, as described in “Materials and Methods.” C, cells treated as in B were washed once with PBS and lysed by sonication in KPi buffer [50 mM KPi buffer, 1 mM EDTA (pH 7.4) containing 20% glycerol]. Cell lysates (30 μ g protein) were analyzed for CYP2B6 protein by Western blotting, as described in “Materials and Methods.”

PC-3 cells with Onyx-017 (Fig. 7B). A more modest increase in CPA toxicity was seen after Adeno-P450 + Onyx-017 coinfection of the aldehyde dehydrogenase-rich A549 cells [Fig. 7C] compare \sim 15% A549 cell kill at 0.5 mM CPA with 12 MOI Adeno-P450 + 2 MOI Onyx-017 versus \sim 70% PC-3 cell kill (Fig. 7B) under the same conditions], despite the efficient expression of P450 and high cellular CPA 4-hydroxylase activity (compare Fig. 6). These experiments were carried out under conditions where the intrinsic adenoviral toxicity was marginal, as judged by the near-absence of an effect of infection with Onyx-017 and Adeno-P450 in the absence of CPA treatment (\leq 12% cell death at Onyx-017 MOI 3 in the experiments shown in Fig. 7). Thus, the substantial cytotoxicity of CPA seen in Fig. 7 is a reflection of *bona fide* prodrug activation-associated cytotoxicity, which, in turn, is a direct result of the helper effect of Onyx-017.

Onyx-017 Enhances Spread of Adeno-P450 in Tumor Xenografts *in Vivo*. We next investigated whether Onyx-017 could be used to enhance the intratumoral spread of Adeno-P450 in A549 and PC-3 xenografts grown s.c. in scid mice. Tumors were grown to approximately 200–300 mm³ in size, at which time they were injected with Adeno-P450 alone, or with Adeno-P450 + Onyx-017 in combination, with each virus given as a series of 5 daily intratumoral injections of 5×10^7 pfu. Tumors were excised 2, 7, or 14 days after the last virus injection and analyzed for CYP2B6 immunostaining after cryosectioning. Fig. 8 shows that the expression of CYP2B6 was largely restricted to small patches of cells in the Adeno-P450-infected A549 tumors (Fig. 8, A and B, left). Little or no P450 expression was detected in Adeno-P450-infected PC-3 tumors (Fig. 8, A and B, right).

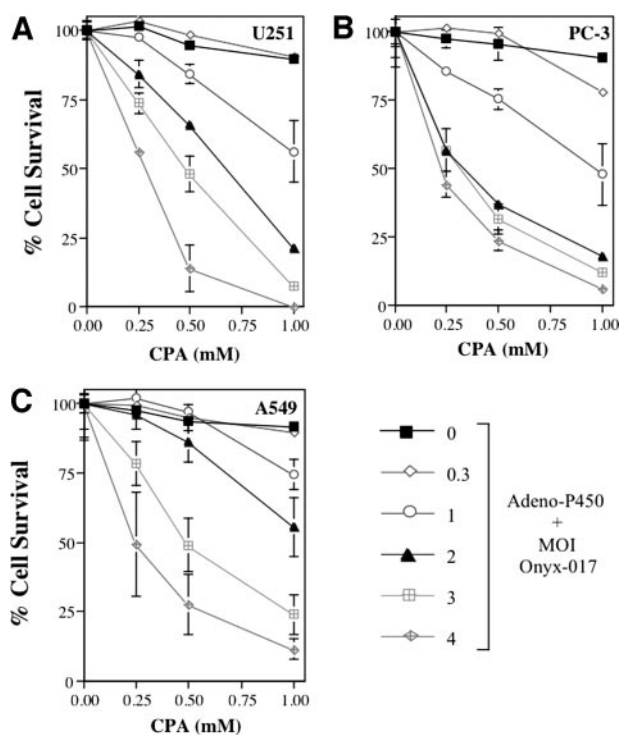


Fig. 7. Enhanced chemosensitivity of U251, PC-3, and A549 cells on coinfection with Adeno-P450 and Onyx-017. A549, PC-3, and U251 cells were infected with Adeno-P450 [multiplicity of infection (MOI) 12 for PC-3 and A549, or MOI 3 for U251, alone or in combination with Onyx-017 at MOIs of 0, 0.3, 1, 2, 3, and 4]. Cells were treated with 0, 0.25, 0.5, or 1 mM cyclophosphamide (CPA) beginning 24 h after infection. The medium was replaced with medium containing fresh CPA (but no virus) 2 days later to remove any infectious viral particles released into the medium, and thereby minimize the intrinsic cytotoxicity of the virus combination in the absence of CPA treatment (e.g., $\leq 12\%$ cell death at Onyx-017 MOI 3 at 0 mM CPA in A–C; data not shown). The cells were then incubated for a total of 7 days of CPA treatment, and then were stained with crystal violet and quantitated. Data are expressed as percentage of survival compared to the corresponding drug-free controls. Data shown are mean \pm half the range values ($n = 2$) and are representative of at least three independent experiments.

P450 expression persisted through the 14-day time point in the A549 tumors, but without spreading to additional tumor cells. By contrast, in the case of both the A549 and the PC-3 tumors coinfecting with Adeno-P450 + Onyx-017, CYP2B6 protein was detected as early as 2 days after the last virus injection (Fig. 8C) and then spread in a time-dependent manner to encompass much larger numbers of tumor cells distributed over a relatively large area (Fig. 8, D–F). Western blotting carried out with PC-3 tumor cell extracts confirmed the much higher overall degree of P450 expression in the Onyx-017 coinfecting tumors (Fig. 9). Large areas of both tumor types in the 14-day coinfection groups showed specific staining for CYP2B6 protein in cells that appeared to lack nuclei, as visualized at higher magnification (Fig. 8F). This may reflect the intrinsic tumoricidal and lytic activity of the replicating Onyx adenovirus, which is known to induce cell death via apoptosis and nuclear disintegration.

Impact of Adeno-P450 in Combination with Onyx-017 on CPA Antitumor Activity in PC-3 Tumor Xenografts. To evaluate the impact of the Onyx-017 helper system on intratumoral prodrug activation and antitumor activity *in vivo*, PC-3 prostate tumors were implanted s.c. in *scid* mice at each posterior flank. Beginning 28 days later, Adeno-P450 and/or Onyx-017 was injected intratumorally using the same viral doses and 5-day injection schedule used in Fig. 8, above. Five days after the last virus injection, mice were treated with CPA using a metronomic schedule consisting of 140 mg CPA/kg body weight repeated every 6 days. Relative tumor volumes referenced to day 35 (2 days before first CPA injection) are presented in Fig. 10.

Untreated PC-3 tumors showed an ~ 6 -fold increase in tumor volume over a 20-day period (days 35–55), after which the mice were killed. CPA-treatment restricted growth of the PC-3 tumors to a 2.5-fold increase in volume over the same time period, consistent with the intrinsic responsiveness of PC-3 tumor cells to activated CPA (compare Fig. 3A) and the therapeutic effectiveness of the metronomic CPA schedule in the context of liver P450-catalyzed CPA activation (21). However, the initial growth-inhibitory response to CPA was followed by stabilization of tumor growth throughout the remainder of the study (day 76), with no consistent tumor regression apparent. Growth of the Adeno-P450-injected and CPA-treated PC-3 tumors was limited to a $\sim 70\%$ increase in tumor volume after seven CPA injections, evidencing an increase in therapeutic response associated with intratumoral, Adeno-P450-dependent CPA activation in comparison to the CPA alone treatment group. PC-3 tumors injected with Adeno-P450 in combination with Onyx-017 exhibited the most dramatic responses to CPA treatment: a sustained, time-dependent tumor regression began by the third CPA injection, decreasing the tumor volume by 37% from its peak value on day 49 (decrease from 135% relative tumor volume on day 49 to 85% on day 76). By contrast, CPA stabilized tumor growth but did not induce detectable tumor regression over the course of the study in the Onyx-017 alone treatment group. No significant toxicity beyond that of CPA treatment alone was associated with virus administration in any of the experimental groups, as determined by monitoring body weight profiles (Fig. 10, legend).

DISCUSSION

P450-based GDEPT is most efficacious when *P450* is delivered to tumor cells in combination with *P450R* (15, 38). This combination not only increases the catalytic activity of the *P450* transgene, it also facilitates the incorporation of bioreductive prodrugs activated by P450 and/or P450R into P450 GDEPT strategies (18). Presently we show that P450 GDEPT is more effective when the *P450-P450R* gene couple, comprised of *CYP2B6* and *P450R*, is delivered to tumor cells via a single viral vector that enables their coordinate expression using an IRES sequence. Functional studies using retroviral and adenoviral vectors demonstrated the intrinsic advantage of the *P450-IRES-P450R* bicistronic construct, which delivers both transgenes to the same cell and results in strong gene transduction in a single infection. *CYP2B6* was found to be a highly suitable candidate for incorporation into an IRES-*P450R* expression cassette, insofar as it is compatible with strong expression of both transgenes from the bicistronic construct and can be delivered either using retrovirus or using a replication-defective adenovirus designated Adeno-P450. By contrast, using a *P450-IRES-P450R* cassette of the same design, *CYP2C19* conferred much weaker CPA cytotoxicity, whereas *CYP2C18* was inactive. We previously encountered difficulties obtaining high-level expression of *CYP2C18* in 9L cells (15), which may help explain the inability of the *CYP2C18-IRES-P450R* expression cassette to sensitize 9L cells to CPA in the present study. Moreover, the poor expression of P450R by this retrovirus construct suggests that the *CYP2C18* cDNA sequence may destabilize the retroviral mRNA. This conclusion is supported by deletion analysis, which localized the *CYP2C18* destabilizing element(s) to a ~ 280 nucleotide 3'-segment of the *CYP2C18* cDNA (1471–1751).¹

The replication-defective Adeno-P450 virus was shown to sensitize a wide range of human tumor cell lines to CPA. However, relatively high doses of this virus were required, and limited infectivity and/or limited *CYP2B6* and *P450R* gene transfer was observed in several of

¹ Unpublished observations.

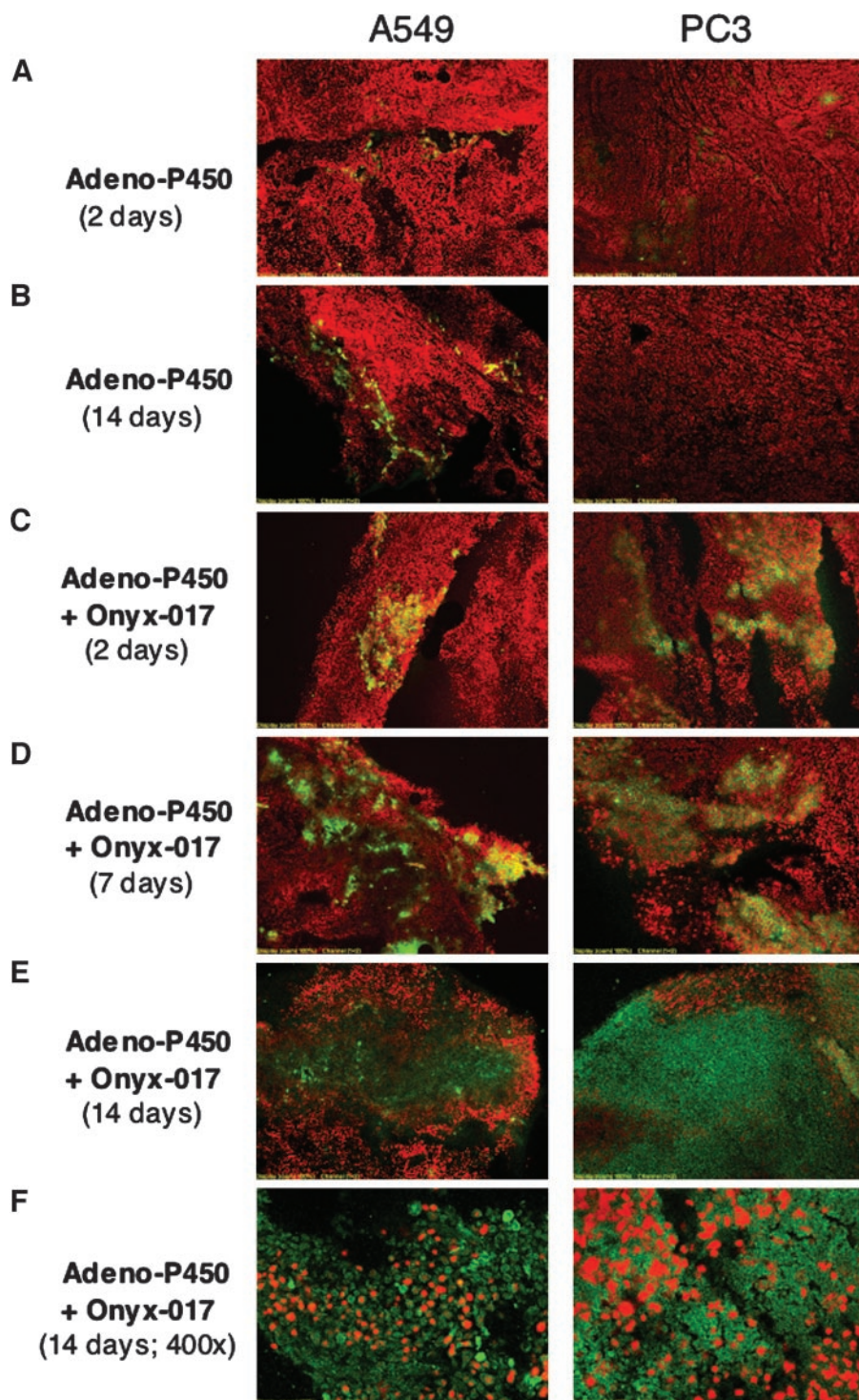


Fig. 8. Onyx-017 enhances tumor cell spread of Adeno-P450 in A549 and PC-3 tumor xenografts. *Scid* mice were inoculated at each posterior flank with 4×10^6 A549 or PC-3 tumor cells as described in "Materials and Methods." Tumors were grown to approximately 200–300 mm³ and then treated with Adeno-P450, alone or in combination with Onyx-017, as indicated, as a series of 5 daily intratumoral injections (5×10^7 plaque-forming units of each virus/injection) as described in "Materials and Methods." Tumors were excised 2 days (A and C), 7 days (D), or 14 days after the last virus injection (B, E, and F), and then cryosectioned. Shown are representative patterns of the expression of CYP2B6 protein (green) and propidium iodide-stained cell nuclei (red) at magnifications of $\times 100$ (A–E) and $\times 400$ (F). A549 cells are shown in the left set of panels; PC-3 cells in the right set of panels. A, CYP2B6 expression limited to small patches of cells; B, limited CYP2B6 expression seen in A549 tumors only; C, CYP2B6 expression more widespread than in A, but still localized. The increase in expression compared to A is particularly striking for the PC-3 tumors; D, CYP2B6 spreads to include additional regions of the tumor compared to C; E, CYP2B6 expression has spread to encompass large sections of the tumor; F, higher magnification of sections shown in E, indicating strong CYP2B6 expression in regions apparently devoid of propidium iodide-stained nuclei (red).

the tumor cell lines tested, notably PC-3 prostate and HT-29 colon carcinoma cells. Furthermore, one of the cell lines studied, A549 lung carcinoma, although infectable by Adeno-P450, was nevertheless insensitive to CPA, most likely due to its high aldehyde dehydrogenase content (36) and the associated intrinsic resistance to activated CPA (Fig. 3). These limitations could largely be overcome by infecting the tumor cells with Adeno-P450 in combination with the tumor cell-replicating adenovirus Onyx-017, which acts as a helper virus and substantially increased expression of the *P450* transgene and conversion of CPA to its active 4-hydroxy metabolite. Remarkable increases in CPA cytotoxicity could thus be achieved, both in tumor cells that

displayed low apparent intrinsic adenoviral infectivity (PC-3 cells) and in cells showing intrinsic resistance to activated CPA (A549 cells). Other experiments demonstrated that the replication-conditional Onyx-017 promotes the coamplification and tumor cell spread of the prodrug-activating Adeno-P450, as seen in cell culture studies and in human tumor xenografts grown in *scid* mice *in vivo*. Onyx-017, like the closely related Onyx-015 in clinical development (39), is an E1b-55k-deleted adenovirus that can efficiently replicate in, and spread from tumor cells that have a deficiency in p53 or in a p53 pathway factor (24, 25). The cancer therapeutic potential of these tumor cell-replicating viruses is considerable, given the p53 pathway defects present in an estimated

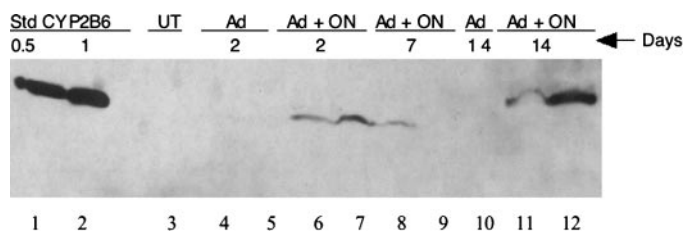


Fig. 9. Adeno-P450 expression in Onyx-017 coinfecting PC-3 tumors. PC-3 tumors were grown in *scid* mice and infected with Adeno-P450 (*Ad*) alone or in combination with Onyx-017 (*ON*), as described in Fig. 8. Extracts were prepared from individual tumors excised on days 2, 7, and 14 after the last viral injection, as indicated, and analyzed on the Western blot shown in the figure (70 μ g protein/well) using mouse anti-CYP2B6 monoclonal antibody. Lymphoblast-expressed CYP2B6 was used as a standard (0.5 and 1 pmol; left lanes of gel). Samples migrated more rapidly in the wells shown at the center of the Western blot. Some inter-sample variability in P450 protein levels is apparent (e.g., lane 8 versus lane 9; lane 11 versus lane 12).

~90% of human cancers. Moreover, because the replication of Adeno-P450 is entirely dependent on that of Onyx-017, the tumor-specificity that is intrinsic to Onyx-017 is expected to confer tumor-selective targeting of Adeno-P450, and hence, selective activation of the P450 prodrug at the site of the tumor *in vivo*. Finally, because the replication of Onyx-017 is dependent on the p53 pathway deficiency of the infected cells, as noted above, this helper virus targeting approach may be applicable to a wide range of human cancers. This contrasts to the more narrow applicability of oncolytic viruses whose tumor specificity is regulated by tumor-specific promoters, such as prostate-specific antigen promoter, which can be used to restrict adenoviral E1a expression and viral replication to prostate cells (40, 41), and α -fetoprotein promoter, used to target hepatocellular carcinomas (42).

Replication-defective adenoviruses are likely to have limited utility for delivery of prodrug-activating enzymes in a clinical setting *in vivo*. Viral particles administered systemically are rapidly cleared from the bloodstream, whereas those introduced by direct intratumoral injection typically remain trapped at the site of injection (43). The replication capability of oncolytic viral vectors, such as the Onyx viruses, may help overcome these problems, as indicated by their effectiveness in gene therapy treatments for cancer, in particular when combined with traditional chemotherapeutic drugs. Onyx-015 has demonstrated efficacy in combination with cisplatin-based chemotherapy (44), and other replicating adenoviruses have demonstrated improved activity in combination with prodrug-activation genes, such as HSV-tk or cytosine deaminase (45–47). These approaches may ultimately be limited, however, by the inhibitory effects of the activated prodrug on replication of the oncolytic viral vector. This may be of particular concern with anticancer prodrugs such as ganciclovir and 5-fluorocytosine, which are converted to antimetabolites that block DNA replication, including viral DNA replication. As a result, antimetabolite-generating prodrugs must be administered after the virus has successfully spread to the target tumor cells (48, 49). In contrast to the antimetabolite prodrugs, however, the low frequency of DNA cross-linking induced by P450-activated CPA suggests that this prodrug is unlikely to inhibit viral replication, a supposition that has been verified in the case of an oncolytic herpes viral vector delivering P450 2B1 (16, 48).

To our knowledge, the present study is the first to use a tumor cell-replicating adenovirus as a helper virus to enhance tumor cell delivery of a prodrug activation gene. These studies confirm and extend earlier reports using replication-conditional adenoviruses to promote the spread of replication-defective adenovirus encoding interleukin 12 or reporter genes such as luciferase or green fluorescent protein (50, 51). Helper virus systems based on the use of two herpes simplex virus amplicons have been described (52, 53), and similar approaches may be used to facilitate the spread of adeno-associated virus armed with suicide or other therapeutic genes. Although a

therapeutic gene, such as P450, could in principle be incorporated directly into the genome of the replicating adenovirus, there are several advantages to using separate viral vectors as described here. First, the two-virus strategy increases the overall gene capacity of the adenoviral delivery system. Second, the ability to infect tumor cells with multiple adenoviral particles makes it possible to use the present helper virus system to deliver two or more therapeutic genes, each encoded by a different adenovirus, thus eliminating the need to engineer all of the requisite sequences into a single adenoviral construct. More complex, regulated therapeutic gene constructs can, therefore, be engineered into individual replication-defective adenoviruses without the need to modify the helper virus. Third, the use of a single vector strategy may potentially dampen and ultimately extinguish adenoviral spread as a result of the linkage between viral-induced cell lysis and cytotoxicity resulting from prodrug activation. This possibility is made even more likely in cases where the prodrug is administered continuously or frequently, such as with the metronomic CPA treatment schedule used in the present study. By contrast, the two-virus system provides for some control over the kinetics of

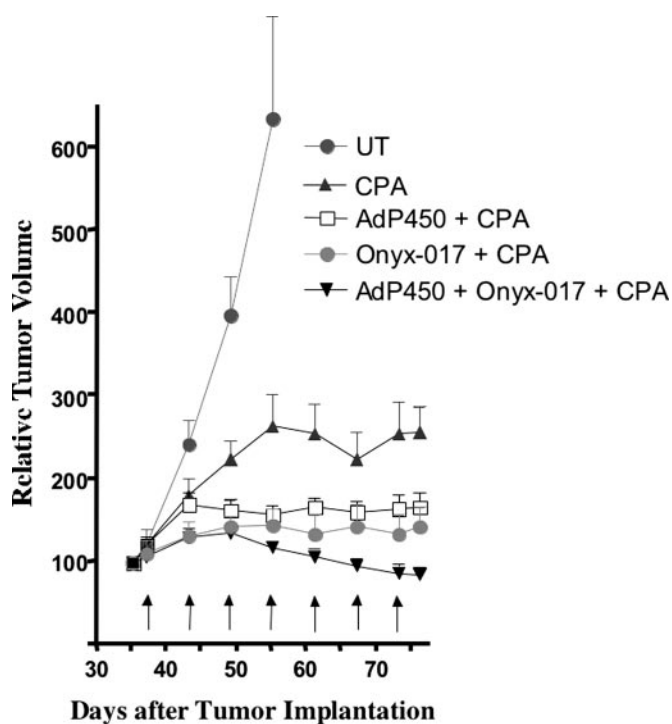


Fig. 10. Tumor growth delay assay: PC-3 xenografts in *scid* mice. *Scid* mice were inoculated with PC-3 tumor cells as in Fig. 8. Tumors were treated with Adeno-P450, alone or in combination with Onyx-017, as indicated, as a series of 5 intratumoral injections beginning 28 days later. Mice were untreated (*UT*) or were treated with 140 mg cyclophosphamide (CPA)/kg body weight every 6 days beginning on day 37; days of CPA injection are marked by vertical arrows along the X axis. Data shown are tumor volumes normalized to the volume of each tumor on day 35, *i.e.* 1 week after the first virus injection, to highlight tumor responses to CPA treatment. Data are based on $n = 5-7$ tumors in each of the five indicated treatment groups (mean; bars, \pm SE). CPA-induced tumor regression was apparent in 6 of the 7 tumors in the Adeno-P450 + Onyx-017 treatment group but not in any of the individual tumors in the other treatment groups (data not shown). The divergence in tumor growth rates between the two Onyx-017-injected groups versus the Adeno-P450 alone-injected group was apparent beginning at day 37 and reflects Onyx-017-dependent antitumor activity. The divergence between the Adeno-P450 + Onyx-017 versus Onyx-017 alone group was apparent beginning at day 49, and reflects the added impact of intratumoral CPA activation. One-way ANOVA analysis of tumor volume data with Bonferroni multiple test correction gave the following significance values: $P < 0.01$ for untreated versus CPA group and $P < 0.001$ for untreated versus all other groups; analysis of the data from days 55–76 gave $P < 0.05$ for Adeno-P450 + CPA versus Onyx-017 + CPA, and $P < 0.001$ for all other pair-wise comparisons. Percentage of decrease in body weight over ~50-day observation period beginning on day of first adenovirus injection (day 28): CPA alone group, $10.7\% \pm 1.3\%$; Adeno-P450 + CPA, $6.3\% \pm 1.6\%$; Adeno-P450 + Onyx-017 + CPA, $8.5\% \pm 1.8\%$; Onyx-017 + CPA, $14.8 \pm 1.9\%$, based on $n = 4$ mice per treatment group.

viral transmission and therapeutic gene spread by varying the ratio of viral particles carrying the replicating, oncolytic virus to viral particles bearing the therapeutic gene. Moreover, using the two-virus strategy, a complete cycle of viral replication may proceed in the absence of the prodrug-activating enzyme in at least some tumor cells within the overall population, thereby propagating viral spread. Fourth, the Onyx-017-based helper system allows for the combination of two independent and complementary strategies for tumor targeting, host cell p53⁺ status to limit replication of the E1b-55k-deleted replicating Onyx virus, and introduction of a tumor-specific transcriptional control element to regulate expression of the therapeutic gene encoded by the replication-defective adenovirus. Finally, the two-virus approach will facilitate much-needed head-to-head comparisons between the Onyx virus and other tumor cell-selective replicating adenoviruses (54) with respect to their ability to deliver, and sensitize tumor cells to, suicide and other therapeutic genes for cancer treatment.

In this regard, Onyx-017 may present several important advantages over other replicating adenoviruses. First, the closely related Onyx-015 virus has shown human safety and encouraging antitumor activity in combination with chemotherapy in multiple clinical trials (55). Second, the intact E3 region present in the Onyx-017 may provide for preferential replication of the E3 (and E1)-deleted Adeno-P450 virus. This possibility is suggested by the finding that E3-deleted adenovirus replicates at ~10-fold higher efficiency than E3 wild-type adenovirus in coinfection studies (56). Third, the Onyx virus has a slow lytic cycle compared with wild-type adenovirus, which may increase the desired tumor cell spread of the replication-defective adenovirus. Other studies suggest, however, that the replication potential and oncolytic activity of the E1b-55k-deleted Onyx virus may be suboptimal in certain p53-deficient tumor cells (57). Oncolytic adenoviruses of which tumor-selectivity is based on mechanisms distinct from that of Onyx-017 (58, 59) may be useful in such cases to facilitate therapeutic gene delivery.

Several potential disadvantages to using the two viral vector system described here should be noted. First, the need to successfully coinfect the same cell target with two separate viruses could present a problem for tumor cells with low intrinsic susceptibility to adenoviral infection due to the absence or low-level expression of integrins, or the adenoviral receptor CAR. Second, recombination between the replicating helper virus and the replication-defective adenovirus may occur and could potentially generate new viruses of which the safety profile is unknown. Third, although a comparatively low dose of adenovirus was used in the present intratumoral injection studies (5×10^8 total pfu), much higher viral doses will likely be required for clinical applications involving systemic virus administration to target metastatic tumors. The potential host toxicities associated with high adenovirus doses may be alleviated, however, by using adenoviruses that contain modified fiber knob protein sequences, which can decrease adenovirus infectivity of host tissues such as the liver and increase the infectivity of CAR receptor-negative cells up to 1000-fold (60).

Finally, while not a factor in the present *scid* mouse study, the immunogenicity of adenoviruses is a critical issue facing the clinical development of adenovirus-based oncolytic viruses (61, 62), in part because of the presence of pre-existing neutralizing antibodies to adenovirus in many patients (63) and because of the need to administer the viral vectors repeatedly and via a systemic route. Antiviral cytotoxic T lymphocytes may, however, contribute to the anticancer response by targeting and thereby destroying adenovirus-infected tumor cells. Modulation of T-cell response and preventing neutralizing antibodies from reaching critical levels might both be possible in the case of CPA-based P450 gene therapies as a consequence of the established immune suppressive activity of CPA and its ability to prevent antigen proliferation of T cells by inducing cytotoxic T-lymphocyte apoptosis (64). This property of CPA may reduce the

immune barrier to adenovirus treatment, as shown by the effectiveness of CPA at inhibiting neutralizing antibodies (65, 66), and increasing and prolonging transgene expression (67, 68). Finally, the wild-type E3b region gp19k gene present in Onyx-017, but not Onyx-015, may inhibit MHC class I antigen presentation (69) and thereby block premature immune elimination of Onyx-017- and Adeno-P450-producing tumor cells.

In summary, the present study describes the use of a wild-type E3 region, tumor cell replication-conditional adenovirus as a helper virus to promote tumor cell spread of Adeno-P450, a replication-defective adenovirus armed with the P450 prodrug-activating genes *CYP2B6* and *P450R*. This combination helps compensate for the poor gene transfer observed with certain human tumor cell lines, greatly increases tumor cell-catalyzed CPA activation, and dramatically enhances the overall sensitization of human tumor cells and tumor xenografts to CPA. The implementation of this strategy for tumor cell targeting of adenoviral vectors may lead to increased activity, enhanced selectivity, and improved delivery of P450 and other therapeutic genes for cancer treatment.

ACKNOWLEDGMENTS

We thank Chong-Sheng Chen for assistance with 4OH-CPA analysis.

REFERENCES

- Aghi, M., Hochberg, F., and Breakefield, X. O. Prodrug activation enzymes in cancer gene therapy. *J. Gene Med.*, 2: 148–164, 2000.
- Kim, D., Niculescu-Duvaz, I., Hallden, G., and Springer, C. J. The emerging fields of suicide gene therapy and virotherapy. *Trends Mol. Med.*, 8: S68–73, 2002.
- McCormick, F. Cancer gene therapy: fringe or cutting edge? *Nat. Rev. Cancer*, 1: 130–141, 2001.
- Wei, M. X., Tamiya, T., Chase, M., Boviatsis, E. J., Chang, T. K. H., Kowall, N. W., Hochberg, F. H., Waxman, D. J., Breakefield, X. O., and Chiocca, E. A. Experimental tumor therapy in mice using the cyclophosphamide-activating cytochrome P450 2B1 gene. *Hum. Gene Ther.*, 5: 969–978, 1994.
- Chen, L., and Waxman, D. J. Intratumoral activation and enhanced chemotherapeutic effect of oxazaphosphorines following cytochrome P450 gene transfer: development of a combined chemotherapy/cancer gene therapy strategy. *Cancer Res.*, 55: 581–589, 1995.
- Chen, L., and Waxman, D. J. Cytochrome P450 gene-directed enzyme prodrug therapy (GDEPT) for cancer. *Curr. Pharm. Des.*, 8: 1405–1416, 2002.
- Jounaidi, Y. Cytochrome P450-based gene therapy for cancer treatment: from concept to the clinic. *Curr. Drug Metab.*, 3: 609–622, 2002.
- Schwartz, P. S., and Waxman, D. J. Cyclophosphamide induces caspase 9-dependent apoptosis in 9L tumor cells. *Mol. Pharmacol.*, 60: 1268–1279, 2001.
- Karle, P., Renner, M., Salmons, B., and Gunzburg, W. H. Necrotic, rather than apoptotic, cell death caused by cytochrome P450-activated ifosfamide. *Cancer Gene Ther.*, 8: 220–230, 2001.
- Chang, T. K. H., Weber, G. F., Crespi, C. L., and Waxman, D. J. Differential activation of cyclophosphamide and ifosfamide by cytochromes P450 2B and 3A in human liver microsomes. *Cancer Res.*, 53: 5629–5637, 1993.
- Weber, G. F., and Waxman, D. J. Activation of the anti-cancer drug ifosfamide by rat liver microsomal P450 enzymes. *Biochem. Pharmacol.*, 45: 1685–1694, 1993.
- Ayash, L. J., Wright, J. E., Tretyakov, O., Gonin, R., Elias, A., Wheeler, C., Eder, J. P., Rosowsky, A., Antman, K., and Frei, E. I. Cyclophosphamide pharmacokinetics: correlation with cardiac toxicity and tumor response. *J. Clin. Oncol.*, 10: 995–1000, 1992.
- Thigpen, T. Ifosfamide-induced central nervous system toxicity. *Gynecol Oncol.*, 42: 191–192, 1991.
- Chen, L., Waxman, D. J., Chen, D., and Kufe, D. W. Sensitization of human breast cancer cells to cyclophosphamide and ifosfamide by transfer of a liver cytochrome P450 gene. *Cancer Res.*, 56: 1331–1340, 1996.
- Jounaidi, Y., Hecht, J. E. D., and Waxman, D. J. Retroviral transfer of human cytochrome P450 genes for oxazaphosphorine-based cancer gene therapy. *Cancer Res.*, 58: 4391–4401, 1998.
- Chase, M., Chung, R. Y., and Chiocca, E. A. An oncolytic viral mutant that delivers the CYP2B1 transgene and augments cyclophosphamide chemotherapy. *Nat. Biotechnol.*, 16: 444–448, 1998.
- Kan, O., Griffiths, L., Baban, D., Iqbal, S., Uden, M., Spearman, H., Slingsby, J., Price, T., Esapa, M., Kingsman, S., Kingsman, A., Slade, A., and Naylor, S. Direct retroviral delivery of human cytochrome P450 2B6 for gene-directed enzyme prodrug therapy of cancer. *Cancer Gene Ther.*, 8: 473–482, 2001.
- Jounaidi, Y., and Waxman, D. J. Combination of the bioreductive drug tirapazamine with the chemotherapeutic prodrug cyclophosphamide for P450/P450-reductase-based cancer gene therapy. *Cancer Res.*, 60: 3761–3769, 2000.

19. McCarthy, H. O., Yakkundi, A., McErlane, V., Hughes, C. M., Keilty, G., Murray, M., Patterson, L. H., Hirst, D. G., McKeown, S. R., and Robson, T. Bioreductive GDEPT using cytochrome P450 3A4 in combination with AQ4N. *Cancer Gene Ther.*, *10*: 40–48, 2003.
20. Huang, Z., Raychowdhury, M. K., and Waxman, D. J. Impact of liver P450 reductase suppression on cyclophosphamide activation, pharmacokinetics and antitumoral activity in a cytochrome P450-based cancer gene therapy model. *Cancer Gene Ther.*, *7*: 1034–1042, 2000.
21. Jounaidi, Y., and Waxman, D. J. Frequent, moderate-dose cyclophosphamide administration improves the efficacy of cytochrome P-450/cytochrome P-450 reductase-based cancer gene therapy. *Cancer Res.*, *61*: 4437–4444, 2001.
22. Browder, T., Butterfield, C. E., Kraling, B. M., Shi, B., Marshall, B., O'Reilly, M. S., and Folkman, J. Antiangiogenic scheduling of chemotherapy improves efficacy against experimental drug-resistant cancer. *Cancer Res.*, *60*: 1878–1886, 2000.
23. Martinez-Salas, E. Internal ribosome entry site biology and its use in expression vectors. *Curr. Opin. Biotechnol.*, *10*: 458–464, 1999.
24. Bischoff, J. R., Kim, D. H., Williams, A., Heise, C., Horn, S., Muna, M., Ng, L., Nye, J. A., Sampson-Johannes, A., Fattaey, A., and McCormick, F. An adenovirus mutant that replicates selectively in p53-deficient human tumor cells [see comments]. *Science (Wash. DC)*, *274*: 373–376, 1996.
25. Heise, C., Sampson-Johannes, A., Williams, A., McCormick, F., Von Hoff, D. D., and Kim, D. H. ONYX-015, an E1B gene-attenuated adenovirus, causes tumor-specific cytolysis and antitumoral efficacy that can be augmented by standard chemotherapeutic agents [see comments]. *Nat. Med.*, *3*: 639–645, 1997.
26. Yew, P. R., and Berk, A. J. Inhibition of p53 transactivation required for transformation by adenovirus early 1B protein. *Nature (Lond.)*, *357*: 82–85, 1992.
27. Morgenstern, J. P., and Land, H. Advanced mammalian gene transfer: high titre retroviral vectors with multiple drug selection markers and a complementary helper-free packaging cell line. *Nucleic Acids Res.*, *18*: 3587–3596, 1990.
28. Yamano, S., Aoyama, T., McBride, O. W., Hardwick, J. P., Gelboin, H. V., and Gonzalez, F. J. Human NADPH-P450 oxidoreductase: complementary DNA cloning, sequence and vaccinia virus-mediated expression and localization of the CYPOR gene to chromosome 7. *Mol. Pharmacol.*, *36*: 83–88, 1989.
29. Lang, T., Klein, K., Fischer, J., Nussler, A. K., Neuhaus, P., Hofmann, U., Eichelbaum, M., Schwab, M., and Zanger, U. M. Extensive genetic polymorphism in the human CYP2B6 gene with impact on expression and function in human liver. *Pharmacogenetics*, *11*: 399–415, 2001.
30. Pear, W. S., Nolan, G. P., Scott, M. L., and Baltimore, D. Production of high-titer helper-free retroviruses by transient transfection. *Proc. Natl. Acad. Sci. USA*, *90*: 8392–8396, 1993.
31. Finer, M. H., Dull, T. J., Qin, L., Farson, D., and Roberts, M. R. kat: a high-efficiency retroviral transduction system for primary human T lymphocytes. *Blood*, *83*: 43–50, 1994.
32. Monga, M., and Sausville, E. A. Developmental therapeutics program at the NCI: molecular target and drug discovery process. *Leukemia (Baltimore)*, *16*: 520–526, 2002.
33. Huang, Z., and Waxman, D. J. HPLC-fluorescent method to determine chloroacetaldehyde, a neurotoxic metabolite of the anti-cancer drug ifosfamide, in plasma and in liver microsomal incubations. *Anal. Biochem.*, *273*: 117–125, 1999.
34. Huang, Z., Roy, P., and Waxman, D. J. Role of human liver microsomal CYP3A4 and CYP2B6 in catalyzing N-dechloroethylation of cyclophosphamide and ifosfamide. *Biochem. Pharmacol.*, *59*: 961–972, 2000.
35. Mizuguchi, H., Xu, Z., Ishii-Watabe, A., Uchida, E., and Hayakawa, T. IRES-dependent second gene expression is significantly lower than cap-dependent first gene expression in a bicistronic vector. *Mol. Ther.*, *1*: 376–382, 2000.
36. Sreerama, L., and Sladek, N. E. Class 1 and class 3 aldehyde dehydrogenase levels in the human tumor cell lines currently used by the National Cancer Institute to screen for potentially useful antitumor agents. *Adv. Exp. Med. Biol.*, *414*: 81–94, 1997.
37. Ries, S., and Korn, W. M. ONYX-015: mechanisms of action and clinical potential of a replication-selective adenovirus. *Br. J. Cancer*, *86*: 5–11, 2002.
38. Chen, L., Yu, L. J., and Waxman, D. J. Potentiation of cytochrome P450/cyclophosphamide-based cancer gene therapy by coexpression of the P450 reductase gene. *Cancer Res.*, *57*: 4830–4837, 1997.
39. Nemunaitis, J., Khuri, F., Ganly, I., Arseneau, J., Posner, M., Vokes, E., Kuhn, J., McCarty, T., Landers, S., Blackburn, A., Romel, L., Randle, B., Kaye, S., and Kirn, D. Phase II trial of intratumoral administration of ONYX-015, a replication-selective adenovirus, in patients with refractory head and neck cancer. *J. Clin. Oncol.*, *19*: 289–298, 2001.
40. Yu, D. C., Chen, Y., Seng, M., Dille, J., and Henderson, D. R. The addition of adenovirus type 5 region E3 enables calydon virus 787 to eliminate distant prostate tumor xenografts. *Cancer Res.*, *59*: 4200–4203, 1999.
41. Rodriguez, R., Schuur, E. R., Lim, H. Y., Henderson, G. A., Simons, J. W., and Henderson, D. R. Prostate attenuated replication competent adenovirus (ARCA) CN706: a selective cytotoxic for prostate-specific antigen-positive prostate cancer cells. *Cancer Res.*, *57*: 2559–2563, 1997.
42. Hallenbeck, P. L., Chang, Y. N., Hay, C., Golygityl, D., Stewart, D., Lin, J., Phipps, S., and Chiang, Y. L. A novel tumor-specific replication-restricted adenoviral vector for gene therapy of hepatocellular carcinoma. *Hum. Gene Ther.*, *10*: 1721–1733, 1999.
43. Vile, R., Ando, D., and Kim, D. The oncolytic virotherapy treatment platform for cancer: Unique biological and biosafety points to consider. *Cancer Gene Ther.*, *9*: 1062–1067, 2002.
44. Heise, C., Lemmon, M., and Kirn, D. Efficacy with a replication-selective adenovirus plus cisplatin-based chemotherapy: dependence on sequencing but not p53 functional status or route of administration. *Clin. Cancer Res.*, *6*: 4908–4914, 2000.
45. Wildner, O., Blaese, R. M., and Morris, J. C. Therapy of colon cancer with oncolytic adenovirus is enhanced by the addition of herpes simplex virus-thymidine kinase. *Cancer Res.*, *59*: 410–413, 1999.
46. Wildner, O., Morris, J. C., Vahanian, N. N., Ford, H., Jr., Ramsey, W. J., and Blaese, R. M. Adenoviral vectors capable of replication improve the efficacy of HSVtk/GCV suicide gene therapy of cancer. *Gene Ther.*, *6*: 57–62, 1999.
47. Freytag, S. O., Rogulski, K. R., Paielli, D. L., Gilbert, J. D., and Kim, J. H. A novel three-pronged approach to kill cancer cells selectively: concomitant viral, double suicide gene, and radiotherapy. *Hum. Gene Ther.*, *9*: 1323–1333, 1998.
48. Pawlik, T. M., Nakamura, H., Yoon, S. S., Mullen, J. T., Chandrasekhar, S., Chiocca, E. A., and Tanabe, K. K. Oncolysis of diffuse hepatocellular carcinoma by intravascular administration of a replication-competent, genetically engineered herpesvirus. *Cancer Res.*, *60*: 2790–2795, 2000.
49. Lambright, E. S., Amin, K., Wiewrodt, R., Force, S. D., Lanuti, M., Propert, K. J., Litzky, L., Kaiser, L. R., and Albelda, S. M. Inclusion of the herpes simplex thymidine kinase gene in a replicating adenovirus does not augment antitumor efficacy. *Gene Ther.*, *8*: 946–953, 2001.
50. Habib, N. A., Mitry, R., Seth, P., Kuppuswamy, M., Doronin, K., Toth, K., Krajcsi, P., Tollefson, A. E., and Wold, W. S. Adenovirus replication-competent vectors (KD1, KD3) complement the cytotoxicity and transgene expression from replication-defective vectors (Ad-GFP, Ad-Luc). *Cancer Gene Ther.*, *9*: 651–654, 2002.
51. Motoi, F., Sunamura, M., Ding, L., Duda, D. G., Yoshida, Y., Zhang, W., Matsuno, S., and Hamada, H. Effective gene therapy for pancreatic cancer by cytokines mediated by restricted replication-competent adenovirus. *Hum. Gene Ther.*, *11*: 223–235, 2000.
52. Saeki, Y., Fraefel, C., Ichikawa, T., Breakefield, X. O., and Chiocca, E. A. Improved helper virus-free packaging system for HSV amplicon vectors using an ICP27-deleted, oversized HSV-1 DNA in a bacterial artificial chromosome. *Mol. Ther.*, *3*: 591–601, 2001.
53. Fraefel, C., Jacoby, D. R., and Breakefield, X. O. Herpes simplex virus type 1-based amplicon vector systems. *Adv. Virus Res.*, *55*: 425–451, 2000.
54. Nemunaitis, J., and Edelman, J. Selectively replicating viral vectors. *Cancer Gene Ther.*, *9*: 987–1000, 2002.
55. Kirn, D. Oncolytic virotherapy for cancer with the adenovirus dl1520 (Onyx-015): results of phase I and II trials. *Exp. Opin. Biol. Ther.*, *1*: 525–538, 2001.
56. Berkner, K. L., and Sharp, P. A. Generation of adenovirus by transfection of plasmids. *Nucleic Acids Res.*, *11*: 6003–6020, 1983.
57. Dix, B. R., O'Carroll, S. J., Myers, C. J., Edwards, S. J., and Braithwaite, A. W. Efficient induction of cell death by adenoviruses requires binding of E1B55k and p53. *Cancer Res.*, *60*: 2666–2672, 2000.
58. Bauerschmitz, G. J., Barker, S. D., and Hemminki, A. Adenoviral gene therapy for cancer: From vectors to targeted and replication competent agents (Review). *Int. J. Oncol.*, *21*: 1161–1174, 2002.
59. Yoon, T. K., Shichinohe, T., Laquerre, S., and Kasahara, N. Selectively replicating adenoviruses for oncolytic therapy. *Curr. Cancer Drug Targets*, *1*: 85–107, 2001.
60. Koizumi, N., Mizuguchi, H., Hosono, T., Ishii-Watabe, A., Uchida, E., Utoguchi, N., Watanabe, Y., and Hayakawa, T. Efficient gene transfer by fiber-mutant adenoviral vectors containing RGD peptide. *Biochim. Biophys. Acta*, *1568*: 13–20, 2001.
61. Cartmell, T., Southgate, T., Rees, G. S., Castro, M. G., Lowenstein, P. R., and Luheshi, G. N. Interleukin-1 mediates a rapid inflammatory response after injection of adenoviral vectors into the brain. *J. Neurosci.*, *19*: 1517–1523, 1999.
62. Worgall, S., Wolff, G., Falck-Pedersen, E., and Crystal, R. G. Innate immune mechanisms dominate elimination of adenoviral vectors following *in vivo* administration. *Hum. Gene Ther.*, *8*: 37–44, 1997.
63. Chen, Y., Yu, D. C., Charlton, D., and Henderson, D. R. Pre-existent adenovirus antibody inhibits systemic toxicity and antitumor activity of CN706 in the nude mouse LNCaP xenograft model: implications and proposals for human therapy. *Hum. Gene Ther.*, *11*: 1553–1567, 2000.
64. Strauss, G., Osen, W., and Debatin, K. M. Induction of apoptosis and modulation of activation and effector function in T cells by immunosuppressive drugs. *Clin. Exp. Immunol.*, *128*: 255–266, 2002.
65. Smith, T. A., White, B. D., Gardner, J. M., Kaleko, M., and McClelland, A. Transient immunosuppression permits successful repetitive intravenous administration of an adenovirus vector. *Gene Ther.*, *3*: 496–502, 1996.
66. Christ, M., Lusky, M., Stoeckel, F., Dreyer, D., Dieterle, A., Michou, A. I., Pavirani, A., and Mehtali, M. Gene therapy with recombinant adenovirus vectors: evaluation of the host immune response. *Immunol. Lett.*, *57*: 19–25, 1997.
67. Jooss, K., Yang, Y., and Wilson, J. M. Cyclophosphamide diminishes inflammation and prolongs transgene expression following delivery of adenoviral vectors to mouse liver and lung. *Hum. Gene Ther.*, *7*: 1555–1566, 1996.
68. Bouvet, M., Fang, B., Ekmekcioglu, S., Ji, L., Bucana, C. D., Hamada, K., Grimm, E. A., and Roth, J. A. Suppression of the immune response to an adenovirus vector and enhancement of intratumoral transgene expression by low-dose etoposide. *Gene Ther.*, *5*: 189–195, 1998.
69. Bruder, J. T., Jie, T., McVey, D. L., and Kovacs, I. Expression of gp19K increases the persistence of transgene expression from an adenovirus vector in the mouse lung and liver. *J. Virol.*, *71*: 7623–7628, 1997.